DOI 10.1007/s10749-017-0733-z
Power Technology and Engineering *Vol. 50, No. 5, January, 2017*

HYDROTECHNICAL CONSTRUCTION

USING THE MULTILAYER FREE-SURFACE FLOW MODEL TO SOLVE WAVE PROBLEMS

V. A. Prokof'ev[1]

Translated from *Gidrotekhnicheskoe Stroitel'svo*, No. 7, July 2016, pp. 18 – 25.

A method is presented for changing over from a single-layer shallow-water model to a multilayer model with hydrostatic pressure profile and, then, to a multilayer model with nonhydrostatic pressure profile. The method does not require complex procedures for solving the discrete Poisson's equation and features high computation efficiency. The results of validating the algorithm against experimental data critical for the numerical dissipation of the numerical scheme are presented. Examples are considered.

Keywords: wind-driven waves; multilayer model; free surface; nonhydrostatic pressure; three-dimensional flows.

The parameters of wind-driven waves for seaports, offshore structures, sea intakes, and other hydraulic-engineering structures (HES) are usually determined:

— based on the regulations [1, 2], which take approximate account of wave diffraction and refraction, disregarding the bottom topography;

— based on numerical models [3, 4], which also make some assumptions. For example, some well-known numerical models (such as the SWAN spectral wave model) are not phase-resolving and produce incorrect data in the space behind the breakwater [4].

Such important phenomena as the nonlinear interaction of currents and waves were either disregarded or described rather approximately. For example, it was proposed in [4] to use Mike21® software to compute the flow field to then superimpose it on the wave field computed with CGWAVE. It is not quite clear how to do that in solving an essentially nonlinear problem. In [4], it is also pointed out that computing the flow and wave fields within the framework of a single hydrodynamic problem requires excessive computational power and, thus, is hardly feasible today. The extended version of Mike21BW® allows describing both currents and waves based on one- and two-dimensional Boussinesq models, but has limitations on the wavelength/depth ratio [5]. The limitations associated with the use of a Boussinesq-type approximation to take into account the effect of non-hydrostatic pressure are described in [6]. Anyway, the two-dimensional problem statement neglects the three-dimensional features of flow without which the algorithm fails the tests presented below.

Another important aspect is the description of the irregularity of waves and the wave spectrum in the presence of complex bottom topography and shore-protection structures. In these cases, the nonlinear interaction of harmonics in the wave spectrum is of importance as well.

It is recognized that the Russian literature pays inadequate attention to the validation of numerical methods for studying waves, though the foreign literature provides abundance of experimental data and analytical solutions that can be used for validation purposes.

Here, we use a unified multilayer free-surface flow model without resort to the hydrostatic pressure hypothesis and Boussinesq approximation. In other words, we the closed three-dimensional system of hydrodynamic equations is solved. Such models have actively been developed and tested abroad over the last 10 years [6 – 14]. The model allows for:

— different velocity (or direction) of the current at each elevation, i.e., in each of the layers, which are not limited in number;

— real pressure profile (the pressure is different at different points);

[1] B. E. Vedeneev All-Russia Research Institute of Hydraulic Engineering (VNIIG), St. Petersburg, Russia; e-mail: ProkofyevVA@vniig.ru

— forces of friction (with the seabed and free surface);

— viscous terms (usually disregarded in foreign publications on wave problems [8, 14]);

— the Coriolis force;

— the effect of wind on the free surface;

— additional sources of currents at different depths: intakes, outlets, inflows.

Moreover, the model allows for heat transfer, vertical temperature stratification, and the dynamics of ice cover formation and bottom deformation. However, these problems are not among wave problems and will be addressed in a separate paper.

Another application of the unified multilayer free-surface flow model is the simulation of the effect of a solitary wave (soliton or tsunami) on maritime HESs in earthquake regions. Using the ordinary shallow-water equations (or even the multilayer model) with the hydrostatic pressure hypothesis to solve wave problems is unacceptable because such an approximation produces a serrated wave profile with vertical front. Accepting the hydrostatic pressure hypothesis in modeling tsunamis would lead to correct results (that are in agreement with the analytic solutions) only for a long solitary wave [15].

Computational Algorithm

1. For further complication, we will use the single-layer shallow-water model based on the Saint-Venant equations. This model is well-known and was validated against problems with discontinuous solutions (for example, dam-break waves); therefore, we will omit its description. The numerical scheme for the single-layer model with hydrostatic pressure was detailed in [16, 17]. Features of this scheme are its conservatism in mass and momentum, the second order of accuracy in two coordinates and time (Hancock algorithm [18, 19]), capability of dealing with discontinuous solutions (HLLE, Roe, etc. schemes [18]), including the case of flow spreading over the dry bottom. The control volume method is used in plan, where the mesh can be either curvilinear or irregular [19].

2. The next step of detalization is to change over to a multilayer model by partitioning the flow into depth layers, but still assuming hydrostatic pressure profile. This changeover allows considering the different directions of currents at the bottom and free surface when the wind load acts on the surface of an enclosed body of water. Similar multilayer models are widely used by oceanologists, but rarely applied to HESs. The multilayer free-surface flow σ-model with hydrostatic pressure was detailed in [20 – 22]. It incorporates mass and momentum exchange between neighboring fluid layers, but does not permit variation in the layer proportion with time. There are other multilayer models in which the fluid mass in each layer is constant [23, 24] and there is no mass exchange among layers. They also employ the control volume method, but cannot solve even the problem of wind-driven current in an enclosed body of water.

3. The final stage of detalization is the multilayer free-surface flow model with nonhydrostatic pressure. Note that the approach we use to correct the pressure profile can also be applied to ordinary (single-layer) shallow-water models. The method of deriving Poisson's equation for pressure by determining the velocity components at each time step from the momentum balance equations and then substituting them into the continuity equation is well-known. The same is true for deriving the equation for pressure corrections in the case to decomposition of equations [11, 25]. Such an approach was frequently used in combination with σ-coordinates [8, 26] or an other vertical discretization method [14]. Possible problems and limitations are the following.

The chief difficulty is to solve, rather than derive, the discrete Poisson's equation: iteration methods for solving it converge poorly and consume most of the computation time. This requires using rather complex iteration algorithms such as Bi-CGSTAB [7, 9, 14], which is a variation of Krylov's method, or GMRES, which is compared with Bi-CGSTAB in [11] and is incorporated, along with others, into Flow-3D® commercial software (based on the VOF method), its convergence being guaranteed only if the ratio of mash spacings in the directions x, y, z is less than 10.

It is often difficult to use meshes that are irregular (including triangular) in plan.

Improper discretization of the equation for the pressure correction ΔP for σ-schemes may cause convergence problems in the case of flow spreading over the dry bottom.

Not all methods that use hydrostatic pressure profile can deal with discontinuous solutions occurring in problems with break waves and hydraulic jumps.

We attempt here to use the method of successive approximations to determine ΔP, doing without complex algorithms of solving Poisson's equation. We will tend to derive a discrete Poisson's equation for ΔP that converges, i.e., its relative error $\varepsilon \approx 10^{-3} - 10^{-6}$ (depending on the type of problem) is reached, in 10 to 30 (rather than hundreds of) iterations. There should be no additional limitations on the ratio of mesh spacings in x, y, z. The method should not introduce considerable numerical dissipation and should be capable of dealing with discontinuous solutions such as bores (break waves).

The main application of the algorithm presented here is to solve wave problems with adequate accuracy and computational efficiency. We do not mean to compete with Flow-3D®, which has been used by the VNIIG for five years and proved to be effective in analyzing spillway and penstock flows and in solving other problems of applied hydraulics. However, using it to solve wave problems involves difficulties associated with very long computation time and severe requirements to the computation mesh. The module of solving wave problems built in the Mike21BW® software (and, possibly, Mike 3) is based on the Boussinesq approximation, which introduces some limitations on its stability and applicability.

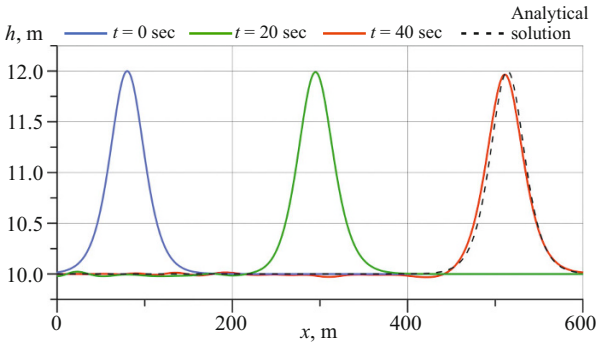

Fig. 1. Propagation of a solitary wave: two-layer model. The dashed line represents the analytic solution for $t = 40$ sec.

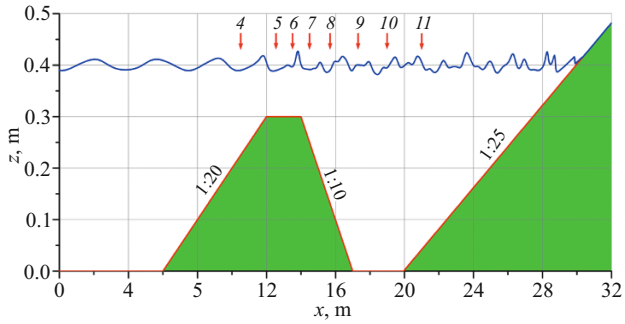

Fig. 2. Schematic of the Beji-Battjes experiment [28]. The figures with arrows indicate the locations of wave gauges.

It is impossible to cover in one paper all the mathematics and numerical algorithm implementing the three hierarchies of the numerical model. A detailed description of the multilayer model and the procedure for correcting the pressure profile can be found not only in [16, 22], but also in [27] where there is also additional video materials. Therefore, we now descend to examples.

Examples of Test Calculations

Propagation of a Solitary Wave (Soliton). This is a typical test always used in similar studies [7, 10, 14]. The analytic solution for the horizontal velocity u and the surface profile η is as follows [12]:

$$c = \sqrt{g(H+h)};\ \varphi = (x - x_0 - ct)\sqrt{\frac{3H}{4h^3}};$$

$$u = \sqrt{gh}\,\frac{H}{h}\,\mathrm{sech}^2(\varphi);\ \ \eta = h + H\,\mathrm{sech}^2(\varphi). \qquad (1)$$

The initial velocity $u(0, t)$ was specified on the left boundary $x = 0$, according to (1). The length of the computational domain was 600 m, and the mesh consisted of 500 nodes. The initial position of the soliton crest $x_0 = 80$ m, the soliton height $H = 2$ m, and the depth $h = 10$ m. The number M of layers was varied from 1 to 12 and weakly affected the results of this example. Figure 1 shows the soliton profiles at different time points for the two-layer model. The dashed line represents the analytic solution for $t = 40$ sec. The oscillations of η behind the soliton are not so high (less than 3 cm) as in many similar calculations [12]. This is owing to the accurate (parabolic) approximation of the pressure profile near the free surface [27]. The hydrostatic approximation cannot be applied to solve this problem [15].

Transformation of a Sinusoidal Wave over a Submerged Obstacle. Beji-Battjes Experiment (Delft, 1993). A schematic of the experiment [28] and the profiles of the free surface at $t = 40$ sec (final second of computation) are shown in Fig. 2. The amplitude of the wave produced by the wave generator (on the left) was equal to 1 cm and its period was 2.02 sec. The bottom on the right had a 1:25 slope and served as a wave absorber. The same bottom was in the numerical model, and, as already mentioned, no problems because of waves running on the dry bank arose during the computations. However, in many foreign studies, such as [10], the bank on the right was replaced by a sponge layer. This test is rather sensitive to numerical dissipation [7]. Therefore, a fine mesh ($\Delta x = 1.25$ cm) was used in [7, 10] to numerically simulate the waves. We used a coarser mesh ($\Delta x = 2$ cm), and the time step (of the order of $\Delta t = 0.0067$ sec) was chosen automatically based on the criterion CFL = 0.9. In this problem, the three-dimensional nature of the flow is manifested as dependence of the results on the number of layers, especially at points 8 – 11 (wave gauges, Fig. 2). At points 8 and 11, the single-layer model, as well as many multilayer models [11], produces results that are far from being in agreement with the experimental data [7, 10]. Figure 3 shows the results obtained with the six-layer model ($M = 6$; uniform partition). At measurement points 4 – 6, the agreement with the experimental data is good even for $M = 2 - 3$.

Transformation of Waves over a Sloped Bottom with an Elliptic Shoal. The previous two tests represented a two-dimensional vertical section of the flow. The third test example is three-dimensional. Its goal was to simulate an experiment (schematized in Fig. 4) on wave propagation over a complex bottom [29]. The blue lines show the initial depths, while the eight lines on which the wave heights were measured are shown in red. In the coordinate system rotated by $\varphi = 20°$

$$x_1 = y\cos\varphi + x\sin\varphi;\ \ y_1 = x\cos\varphi - y\sin\varphi$$

the bottom profile is described by

$$D = \begin{cases} 0, \text{ if} \left(\dfrac{x_1}{4}\right)^2 + \left(\dfrac{y_1}{3}\right)^2 > 1, \\ -0.3 + 0.5\sqrt{1 - \left(\dfrac{x_1}{5}\right)^2 - \left(\dfrac{y_1}{3.75}\right)^2}; \end{cases}$$

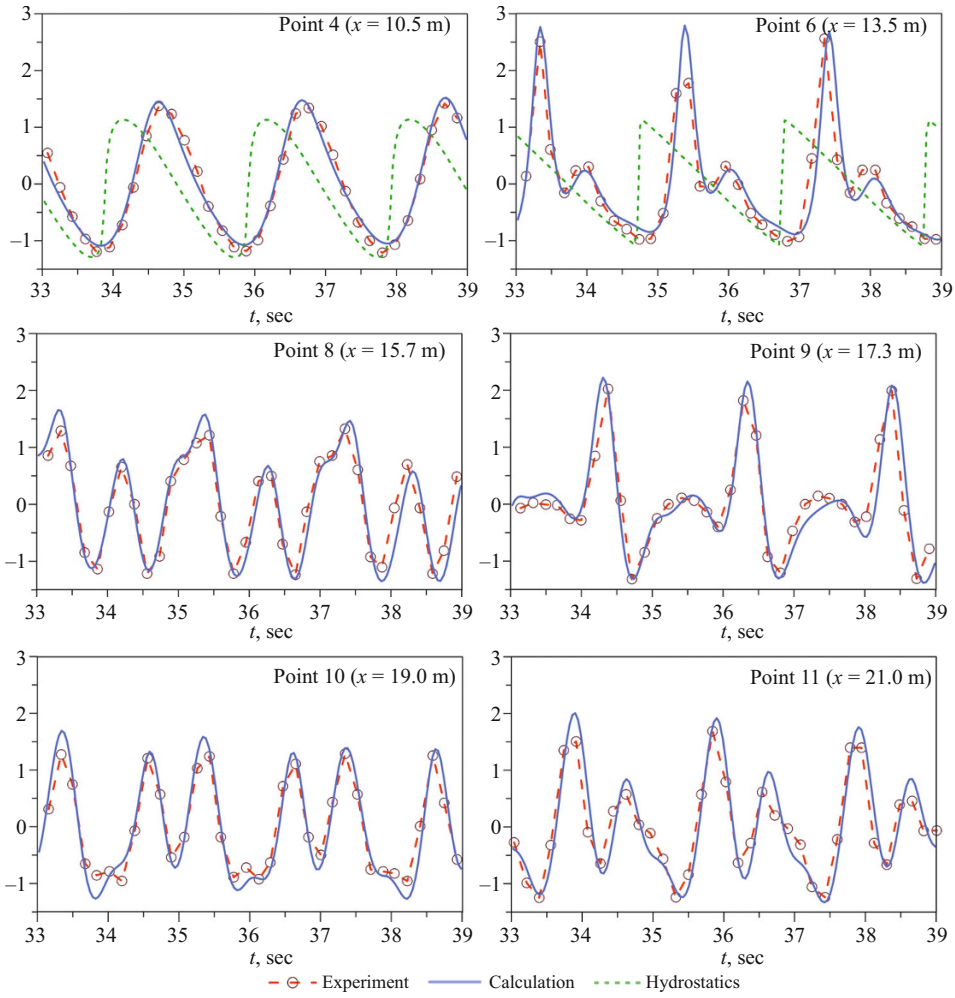

Fig. 3. Comparison of the results calculated with a six-layer model and the data of the Beji-Battjes experiment.

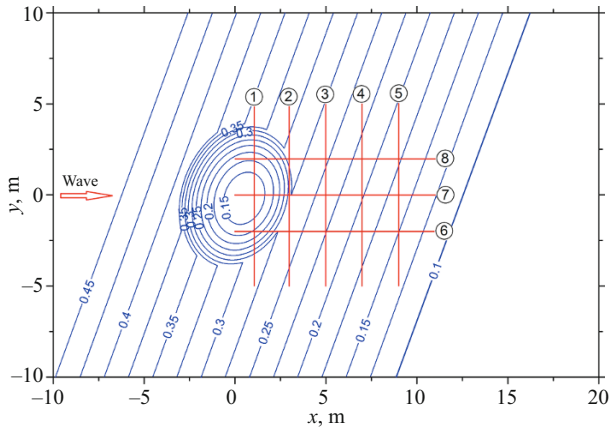

Fig. 4. Schematic of the Berkhoff, etc. experiments [29]. The figures in circles indicate the lines of measurement of wave heights.

$$Z_b(x_1, y_1) = D - \min(0.45, \max[0.1; 0.45 - 0.02(5.84 + y_1)]).$$

The wave generator created a sinusoidal wave of height $H_0 = 2A = 4.64$ cm and period $T = 1.0$ sec. The total time of experiment was 34 sec. It was sufficient for the wave pattern to stabilize, but insufficient for the wave to reach the right boundary. The maximum wave height H (from trough to crest) at each point of the red lines (Fig. 4) was determined during the last four seconds (four wave periods) of the experiment. In the numerical experiment, this corresponded to the determination of the minimum/maximum displacement of the free surface at the measurement points of these lines within each of the last four periods, followed by averaging over the four measurements. The same experimental data were used to validate the numerical models in [7, 14]. It appeared that the accuracy of the results strongly depends on the numerical dissipation of the scheme. For the algorithm presented here, a two-layer model with a 750 × 500 mesh ($\Delta x = \Delta y = 4$ cm; foreign researchers sometimes use $\Delta x = 2.5$ cm) is sufficient. The time step (of the order of $\Delta t = 0.007$ sec) was chosen automatically based on the criterion CFL = 0.75. The wave generator was modeled by harmonic variation in the flow over the entire depth on the left. Slippage boundary conditions were specified on the lateral walls of the basin. Quadratic bottom friction corresponded to the Manning coefficient $n = 0.012$. A no-flow condition was specified on the right boundary, and a sponge layer (which is

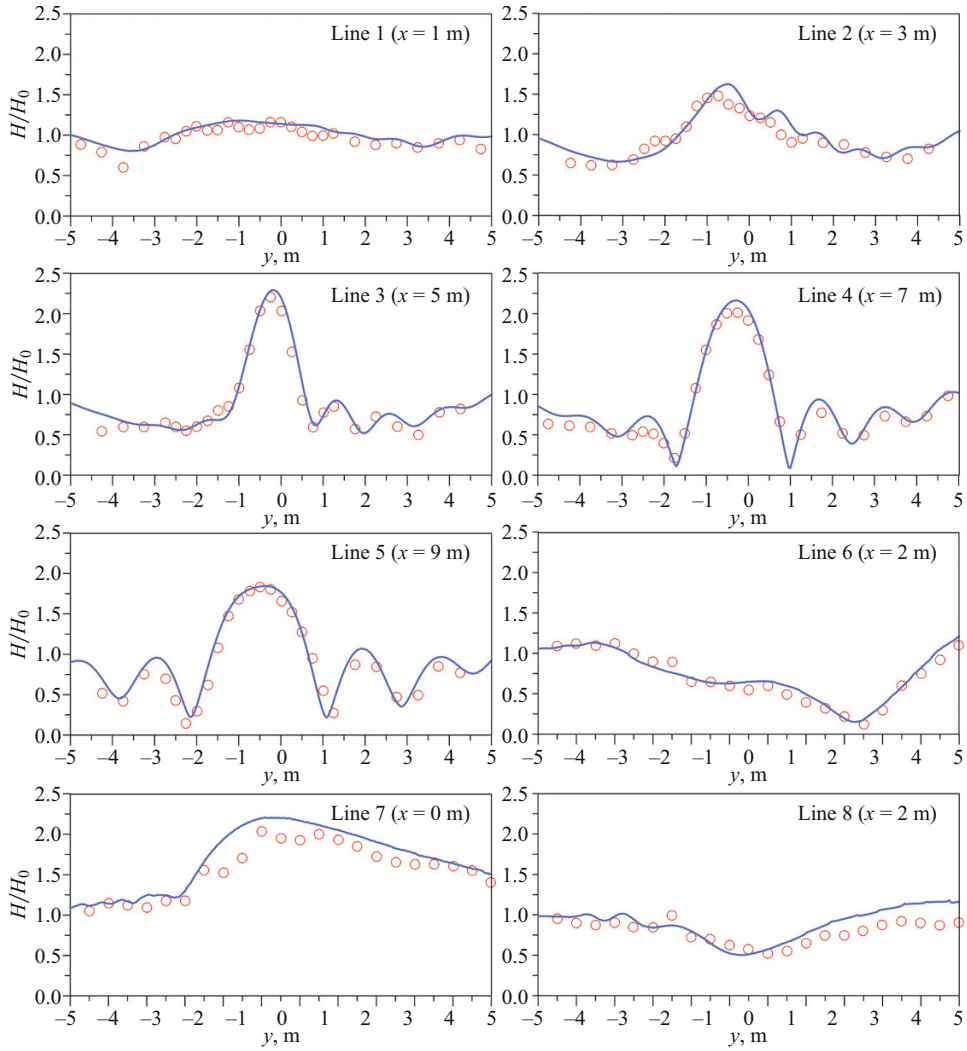

Fig. 5. An elliptic shoal [29]: comparison of calculated results (two-layer model) averaged over the last four periods of wave heights and experimental data.

also used in Mike21BW®) absorbing the energy of the waves was added to the last section of length L = 5 m of the computational domain. The coefficient of additional linear friction on this section is as follows [7]:

$$R_k = \frac{1}{4}\left(1+\tanh\left[\frac{\sin(\pi\delta)}{(1-\delta^2)}\right]\right);$$

$$\tilde{x} = \frac{x - x_{\max} + L}{L};\quad \delta = \begin{cases} 4\tilde{x} - 1, \text{ if } 0.001 < \tilde{x} < 0.5, \\ 3 - 4\tilde{x}, \text{ if } 0{,}5 < \tilde{x} < 0.999. \end{cases}$$

The calculated results are presented in Fig. 5. The maximum wave heights resulting from wave interference (measurement lines 3, 4, 5) are predicted quite accurately. The run time on an ordinary all-in-one PC (four processors) did not exceed 40 min (though the programming language is Delphi), processor utilization was about 98%, and the algorithm was easily parallelized. The results obtained with a mesh twice finer in all three coordinates are also in good agreement with the experimental data.

Calculations for Real Hydraulic-Engineering Structures. Two additional examples were numerically analyzed to test the efficiency (speed) of the software and its stability for complex bottom configurations inherent in real objects.

One example is the S1 navigation pass (with the floating gates open) of the St. Petersburg Flood Protection Barrier (Fig. 6). The computational domain was 929 m along the x-axis (along the wavefront) and 1395 m along the y-axis (along the wave propagation). The mesh consisted of 465 × 448 nodes, and the depth was divided into five layers. The dynamics of the flow (identical on all depth) for generation of irregular waves was specified on the right boundary: five harmonics with different phases and amplitudes and an average wave period of 8 sec, the height (from trough to crest) of a harmonic with this period being 2 m. The left boundary was a wall-the Sommerfeld boundary condition was not specified there. The time of computation for full-scale conditions was 240 sec, and the total time of computation was about 35 min. Despite wave runup on moles and banks, the algorithm remained stable, the time step of the numerical scheme was absolutely stable, and Poisson's equa-

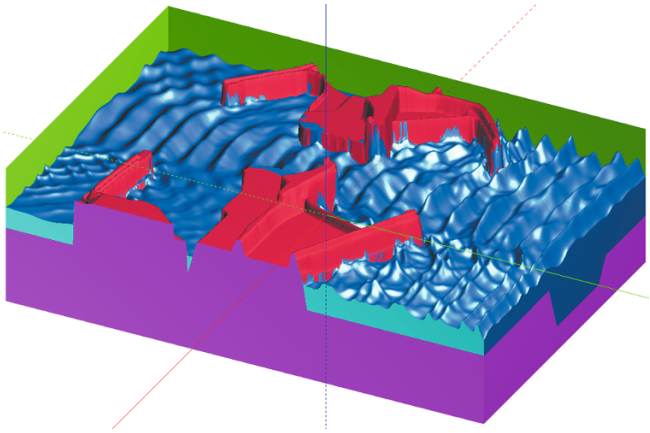

Fig. 6. Transformation of irregular waves in the basin adjacent to the S1 Navigation Pass. The wave generator is on the right.

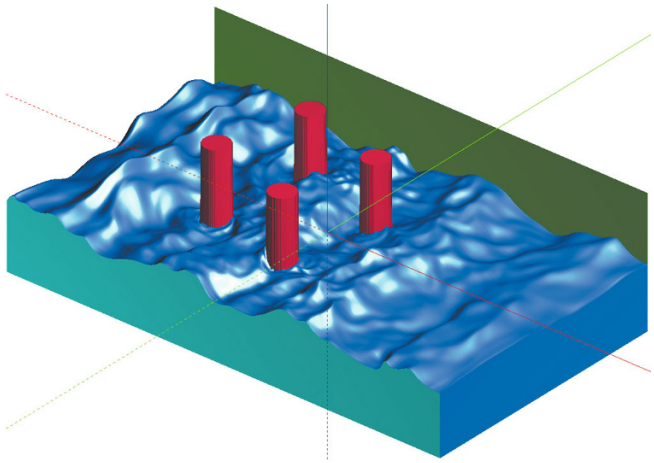

Fig. 7. Action of irregular waves on the footing of an offshore drilling platform. The wave generator is on the left.

tion was solved in 15 iterations even after ten time steps. In the right lower corner of the figure (near the mole), so-called clapotis was observed [4]. Though a wave of medium length covered only 26 nodes of the mesh, it appeared sufficient, as was noticed in solving the test problems (30 to 35 nodes per wavelength is optimal). This is due to the second order of accuracy of the model in coordinates. Disabling this option drastically worsened the accuracy of computation. The waves quickly died away, and the results obtained with coarser and finer mashes were no longer in agreement.

The other example is four cylindrical footings of an offshore drilling platform (Fig. 7). The footings, each of radius 10 m, were located at the corners of a square with a diagonal length of 100 m. The square was turned by 30° to the wavefront arriving from the left. The initial depth was 20 m, and the waves were irregular, as in the previous example (the average period 8 sec; the average wave height 4 m). The wave spectrum is not important for test computations. The computational domain was 200 m in width and 350 m in length, the mesh spacing $\Delta x = \Delta y = 0.3$ m, and the depth was divided into eight layers to determine the wave load on each footing. The Sommerfeld boundary condition was specified on the right boundary (Fig. 7). The wave generator was intentionally placed close to the footings to show how the waves reflected from them alter the wave pattern, even near the left boundary. When numerically solving such problems or when conducting physical experiments in a wave basin, it is, obviously, necessary to place the wave generator at a greater distance to enlarge the modeled domain. Note that the method described here also allows calculating the loads on each of the footing with allowance for the phase, which is important for testing the stability of the whole structure.

CONCLUSIONS

The proposed method of solving wave problems based on the three-dimensional multilayer free-surface flow model has demonstrated high computational efficiency and, what is more, reliability. Not all examples against which it was tested have been presented. All the examples demonstrated the good convergence of the iterative determination of the pressure correction ΔP or the stability of the whole algorithm. The algorithm is of the second order of accuracy in both time and coordinates. This allows solving wave problems sensitive to numerical dissipation. It is not required to select the parameters of the algorithm to solve a specific problem; it is sufficient to select an appropriate mesh. Spreading of the flow over the dry bottom, such as wave run-up on a bank, does not present difficulties. The algorithm can easily be adapted to irregular meshes and parallelized.

The method remains stable even when solving problems of the propagation of a bore or modeling hydraulic jumps. It is planned to conduct a series of computations for similar problems to compare with Flow-3D®. A version of the algorithm is being developed for irregular meshes. The software as it stands can be used to analyze the transformation of wind-driven waves or tsunamis in water areas with complex configuration of the bottom and breakwaters.

REFERENCES

1. *Rules and Regulations SP 38.13330.2012. Loads and Impacts on Hydraulic-Engineering Structures* (*from Waves, Ice, and Ships*). *Actualized Edition of SNiP 2.06.04–82** [in Russian], Izd. Min. Reg. Razvit. RF, Moscow (2013).
2. *Manual on Determination of Loads and Impacts* (*from Wave, Ice, and Ships*) [in Russian], Izd. VNIIG, Leningrad (1977).
3. N. N. Zagryadskaya and S. G. Kalinin, "Numerical modeling of marine-wave propagation on water areas," *Power Technol. Eng.*, **41**(4), 208 – 213 (2007).
4. S. B. Kuklev and B. V. Divinskii, "Some aspects of mathematical simulation of hydrodynamic processes behind breakwaters of artificial lands," in: *Proc. Int. Conf. on Creation and Use of Artificial Grounds on Coasts and in Water Areas* [in Russian], Novosibirsk (2009), pp. 80 – 89.

5. B. V. Divinskii, P. B. Kos'yan, and S. B. Kuklev, "Parameters of wind-driven waves in protected water areas," *Fundam. Prikl. Gidrofiz.*, No. 4 (10), 5 – 16 (2010).
6. G. Stelling and M. Zijlema, "Numerical modeling of wave propagation, breaking and run-up on a beach," in: *Advanced Computational Methods in Science and Engineering. Vol. 1 of Ser. Lecture Notes in Computational Science and Engineering* (2009), pp. 373 – 401.
7. G. Stelling and M. Zijlema, "An accurate and efficient finite-difference algorithm for non-hydrostatic free-surface flow with application to wave propagation," *Int. J. Numer. Meth. Fluids*, **43**, 1 – 23 (2003).
8. G. Stelling and M. Zijlema, "Efficient computation of surf zone waves using the nonlinear shallow water equations with non-hydrostatic pressure," *Coastal Eng.*, **55**, 780 – 790 (2008).
9. M. Zijlema and G. Stelling, "Further experiences with computing non-hydrostatic free-surface flows involving water waves," *Int. J. Numer. Meth. Fluids*, **48**, 169 – 197 (2005).
10. Y. Yamazaki, Z. Kowalik, and K. F. Cheung, "Depth-integrated, non-hydrostatic model for wave breaking and runup," *Int. J. Numer. Meth. Fluids*, **61**, 473 – 497 (2009).
11. S. Ullmann, *Three-Dimensional Computation of Non-hydrostatic Free-Surface Flows. MSc. Thesis*, Delft Univ. of Technology (2008).
12. M. Van Reeuwijk, *Efficient Simulation of Non-hydrostatic Free-Surface Flow. Wave Simulation with Interpolation of the Vertical Pressure Profile. MSc. Thesis*, Delft Univ. of Technology (2002).
13. C-C. Young, C-H. Wu, W-C. Liu, and J-T. Kuo, "A higher-order non-hydrostatic σ-model for simulating nonlinear refraction-diffraction of water waves," *Coastal Eng.*, **56**, 919 – 930 (2009).
14. C. Ai, S. Jin, and B. Lv, "Anew fully non-hydrostatic 3D free surface flow model for water wave motions," *Int. J. Numer. Meth. Fluids*, **66**, 1354 – 1370 (2011).
15. M.-O. Bristeau, N. Goutal, and J. Sainte-Marie, "Numerical simulations of a non-hydrostatic shallow water model," *Comp. Fluids*, **47**(1), 51 – 64 (2011).
16. V. A. Prokof'ev, "Two-dimensional horizontal numerical model of open flow over a bed with obstacles," *Water Resources*, **32**(3), 252 – 264 (2005).
17. V. A. Prokof'ev, "State-of-the-art numerical schemes based on the control volume method for modeling turbulent flows and dam-break waves," *Power Technol. Eng.*, **36**(4), 235 – 242 (2002).
18. A. G. Kulikovskii, N. V. Pogorelov, and A. Yu. Semenov, *Mathematical Aspects of Numerical Solution of Hyperbolic Systems of Equations* [in Russian], Fizmatlit, Moscow (2001).
19. C. G. Mingham and D. M. Causon, "Calculation of unsteady bore diffraction using a high resolution finite volume method," J. *Hydraulic Res.*, **38**(1), 49 – 56 (2000).
20. E. Audusse, M.-O. Bristeau, B. Perthame, and J. Sainte-Marie, "A multilayer Saint-Venant system with mass exchanges for shallow water flows. Derivation and numerical validation," *ESA-IM. M2AN*, **45**(1), 169 – 200 (2011).
21. E. Audusse, M. -O. Bristeau, M. Pelanti, and J. Sainte-Marie, "Approximation of the hydrostatic Navier-Stokes system for density stratified flows by a multi-layer model. Kinetic interpretation and numeral solution," *J. Comput. Phys.*, **230**(9), 3453 – 3478 (2011).
22. V. A. Prokofyev, "Application of unified 3D hydro-thermal model of a reservoir for estimation of HPP construction influence on environment," in: *Proc. Int. Symp. on Dams for A Changing World. Sect. 5*, Kyoto, Japan, June 5 (2012), pp. 69 – 74.
23. F. Benkhaldoun and M. Seaid, "Solving the multi-layer shallow water equations using the finite volume modified method of characteristics," in: *Proc. 5th European Conf. on Computational Fluid Dynamics*, Lisbon, June (2010).
24. E. Audusse and M.-O. Bristeau, "Finite-volume solvers for a multilayer Saint-Venant system," *Int. J. Appl. Math. Sci.*, **17**(3), 311 – 320 (2007).
25. Z. Lai, C. Chen, G. W. Cowles, and R. C. Beardsley, "A nonhydrostatic version of FVCOM: 1. Validation experiments," *J. Geophys. Res.*, **115**, C11010 (2010), DOI: 10.1029/2009JC005525.
26. C-C. Young, C-H. Wu, W-C. Liu, and J-T. Kuo, "A higher-order non-hydrostatic σ-model for simulating nonlinear refraction-diffraction of water waves," *Coastal Eng.*, **56**, 919 – 930 (2009).
27. V. A. Prokof'ev, "Multilayer free-surface flow model: A simple method to determine pressure for wave problems," *Izv. VNIIG*, **278**, 47 – 78 (2015), http://gofile.me/2Zesj/kjZWQXt4
28. S. Beji and J. A. Battjes, "Experimental investigation of wave propagation over a bar," *Coastal Eng.*, **19**, 151 – 162 (1993).
29. J. C. W. Berkhoff, N. Booy, and A. C. Radder, "Verification of numerical wave propagation models for simple harmonic linear water waves," *Coastal Eng.*, **6**, 255 – 279 (1982).